Bioresources and Bioproducts

MDPI

Article

Coffionic Fractionation of Horse Manure: Improving Methane Yield and Enzymatic Lignin Functionalization for Tailored PLA–Lignin Materials

Lindsay Dorschner Pelcoq [1], Fenosoa Tatiana Randremahitsimanana [1,2], Asmina Chanfiou [1,3], Amani Belaiba [1], Lily Dubosquelle [3], Sanae El Moudni El Alami [1], Arash Jamali [4], David Mathiron [5], Catherine Sarazin [1], Caroline Hadad [3] and Eric Husson [1,*]

[1] Unité de Génie Enzymatique et Cellulaire GEC, UMR CNRS 7025, Université de Picardie Jules Verne, 33 rue Saint-Leu, 80039 Amiens, France; catherine.sarazin@u-picardie.fr (C.S.)
[2] Petroleum Engineering Department, Ecole Supérieure Polytechnique d'Antananarivo, University of Antananarivo, Antananarivo BP 1500, Madagascar
[3] Laboratoire de Glycochimie et des Agroressources d'Amiens LG2A, UR 7378, Université de Picardie Jules Verne, 33 rue Saint-Leu, 80039 Amiens, France; caroline.hadad@u-picardie.fr (C.H.)
[4] Plate-Forme de Microscopie Électronique de l'Université de Picardie Jules Verne, UFR Sciences, 33 rue Saint-Leu, 80039 Amiens, France; arash.jamali@u-picardie.fr
[5] Plate-Forme Analytique de l'Université de Picardie Jules Verne, UFR Sciences, 33 rue Saint-Leu, 80039 Amiens, France; david.mathiron@u-picardie.fr
* Correspondence: eric.husson@u-picardie.fr

Abstract

Horse manure is an abundant lignocellulosic feedstock with potential for circular biorefineries to diversify and upgrade the methane value chain. However, integrated fractionation strategies enabling the simultaneous valorization of both polysaccharides and lignin remain poorly explored. Here, we developed the Coffionic strategy, a closed-loop, green iono-organosolv fractionation combining, in a two-step, one-batch approach, the eco-acceptable ionic liquid 1-ethyl-3-methylimidazolium acetate and the food-grade solvent 2-methyltetrahydrofuran-3-one, with full solvent recovery and recycling. This strategy selectively recovered 70% *w*/*w* of the lignin from horse manure, yielding a Coffionic lignin fraction with a purity of 78% *w*/*w* and less than 2.5% *w*/*w* of residual sugars. The resulting polysaccharide-rich fraction showed enhanced enzymatic digestibility, achieving >99% cellulose conversion and increasing the biochemical methane potential by 17% compared with untreated horse manure. Coffionic lignin was further upgraded by enzymatic transesterification using immobilized Novozym435® in the same food-grade solvent employed for fractionation, yielding lignin esters compatible with PLA. Esterified lignin–PLA films reached a total surface energy significantly higher than neat PLA and unmodified lignin–PLA films. Overall, the Coffionic strategy provides an integrated and low-waste biorefinery route enabling the simultaneous production of biomethane and high-value lignin-based materials from horse manure.

Keywords: horse manure; iono-organosolv fractionation; biomethane; enzymatic lignin functionalization; green solvents; PLA composites

Academic Editor: Ronald Charles Sims

Received: 23 July 2026
Revised: 6 August 2026
Accepted: 10 August 2026
Published: 17 August 2026

1. Introduction

In the context of the transition toward a circular bioeconomy, livestock wastes represent a promising source of lignocellulosic biomass for producing bioenergy, biomaterials

and bioproducts while reducing environmental impacts [1]. Global manure production exceeds 3.5 billion tons annually, including about 400 million tons of horse manure [2]. This abundant resource is well suited for local anaerobic digestion plants, as horse manure contains up to 50% *w*/*w* polysaccharides on a dry matter basis [3–5]. However, methane production is limited by lignin, whose content ranges from 9 to 50% *w*/*w* depending on the feedstock, as lignin restricts the accessibility of hydrolytic enzymes and methanogenic microorganisms [6,7]. Thus, the biochemical methane potential (BMP) of horse manure generally ranges between 100 and 200 m^3 $CH_4 \cdot t^{-1}$ OM, which is much lower than that of more readily degradable biomass such as food waste [7,8]. Selective lignin extraction prior to anaerobic digestion could therefore increase methane production while simultaneously generating a high-value lignin fraction. The challenge is therefore to efficiently extract lignin while at least preserving the BMP of the polysaccharide-rich fraction or improving it. Lignin is a complex aromatic and polyphenolic biopolymer based on arrangements of three monolignols: *p*-coumaryl alcohol, coniferyl alcohol, and sinapyl alcohol with various interunit linkages, among which aryl-ether (β-O-4) is the most abundant [9]. Minimizing the cleavage of β-O-4 linkages during fractionation limits lignin condensation while preserving a substantial fraction of the native aliphatic hydroxyl groups, thus ensuring a highly reactive polymer suitable for subsequent modification and valorization [10]. Among the possible valorization routes, the incorporation of lignin into polylactic acid (PLA), one of the leading bio-based polymers for 3D printing, has attracted increasing interest to develop more sustainable composites with enhanced mechanical and functional properties [11]. The preservation of aliphatic hydroxyl groups facilitates the esterification of lignin prior to its incorporation into the PLA matrix, thereby enhancing lignin–PLA compatibility [12]. Chemical esterification is the most common modification route. However, enzymatic catalysis offers a greener and more selective alternative, especially toward aliphatic hydroxyl groups [13–15]. Several sustainable lignin fractionation processes have been widely investigated [16–18]. Each process offers advantages but also limitations. Based on our previous results, ionic liquid pretreatments followed by enzymatic hydrolysis applied to Miscanthus or horse manure allow for the isolation of more than 60% of the initial lignin with a β-O-4 interunit linkage content of approximately 35%. However, the isolated lignin still contains more than 10% *w*/*w* residual sugars [19,20]. In contrast, the revisited organosolv process CoffeeCat, previously developed by our group, yields lignin containing less than 5% *w*/*w* residual carbohydrates and a β-O-4 interunit linkage content of 27–35%. However, lignin recovery remains limited, reaching a maximum of about 40% of the initial lignin [19,21]. These studies illustrate the persistent trade-off between lignin recovery, lignin purity, preservation of aryl-ether interunit linkages and the need for new fractionation strategies capable of simultaneously maximizing these three parameters. To address this challenge, an eco-friendly iono-organosolv fractionation strategy, named Coffionic, was developed. This strategy aims to combine the ability of ionic liquids to disrupt the lignocellulosic matrix and improve the accessibility of biomass polymers with the selective lignin extraction strategy developed in the CoffeeCat process. The Coffionic strategy uses the eco-acceptable ionic liquid 1-ethyl-3-methylimidazolium acetate ([C_2mim][OAc]), the biodegradable food-grade solvent 2-methyltetrahydrofuran-3-one (MeTHF-3-one) and the natural amino acid L-glutamic acid, which acts as a mild bio-based acid catalyst, promoting lignin extraction while avoiding mineral acids [19–22]. To the best of our knowledge, this is the first iono-organosolv strategy specifically developed for horse manure valorization. The polysaccharide-rich fraction and the isolated lignin were thoroughly investigated by chemical analyses, spectroscopic (FTIR and NMR) and microscopic (ESEM) techniques. The enzymatic digestibility and the biochemical methane potential of the polysaccharide-rich fraction were evaluated to determine its relevance as substrate for anaerobic digestion.

https://doi.org/10.3390/bioresourbioprod2030016

Extracted lignin was subsequently subjected to transesterification with long acyl chains catalyzed by the immobilized lipase from Candida antarctica (Novozym®435) in MeTHF-3-one, in line with circularity principles. The resulting lignin derivatives were incorporated into polylactic acid (PLA) films to evaluate the effect of enzymatic functionalization on their compatibility and material properties.

2. Materials and Methods

2.1. Feedstock Composition

Raw horse manure (HM) was collected from the racehorse stables of Chantilly (Hauts-de-France, France) and supplied by SAS-EQUI-ENERGIES (Coye-la-Forêt, Hauts-de-France, France). HM mainly consists of high-density wheat straw from the Crau plain (Provence-Alpes-Côte d'Azur, France) used as bedding, mixed with the feces and urine of horses fed a diet based on Crau PDO hay. Prior to use, HM was freeze-dried using a FreeZone® 2.5 L benchtop freeze dryer (Labconco, Kansas City, MO, USA), then milled in a ball mill (PM 400, Retsch, Niederanven, Luxembourg) for 6 min at 25 s^{-1}, yielding particles with sizes below 800 µm, as confirmed by SEM analysis. The milled biomass was subsequently washed in hot water (70 °C) for 3 h to remove potential inhibitory or denaturing compounds. The chemical composition of HM was determined according to NREL standard protocols [23]. The composition (% *w*/*w*, dry matter basis) was as follows: L-arabinan, 1.12 ± 0.64; D-galactan, 0.45 ± 0.23; D-glucan, 25.37 ± 4.79; D-xylan, 15.40 ± 3.13; and total lignin, 35.44 ± 6.61, comprising acid-soluble lignin (ASL, 16.42 ± 5.84) and acid-insoluble lignin (AIL, 19.32 ± 1.57).

2.2. Chemicals and Enzymes

1-ethyl-3-methylimidazolium acetate ([C_2mim][OAc], >98%) was acquired from Solvionic S.A. (Verniolle, France). MeTHF-3-one or coffee furanone (>97%) and dichloromethane (DCM) were supplied by Alfa Aesar (Lancashire, UK). L-glutamic acid (>99%), D-glucose, D-xylose, L-arabinose, D-galactose, ethyl oleate (98%), *N*-hydroxypthalimide, chromium (III) acetylacetonate, 2-chloro-4,4,5,5-tetra-methyl-1,3,2-dioxaphospholane (TMDP), pyridine (99.8%), deuterated chloroform ($CDCl_3$ > 99.8%), and HPLC grade trifluoroacetic acid (99%) were purchased from Sigma Aldrich (Steinheim, Germany). Sulfuric acid 72% *w*/*w* and dimethyl sulfoxide d6 (99.80%) were obtained from VWR (Rosny-sous-Bois, France). Dimethyl sulfoxide-d_6 (DMSO, 99.80%) was obtained from VWR (Rosny-sous-Bois, France). Glass microfiber filters (<1 µm pore size) were from Whatman, GE Healthcare Life Sciences (Boston, MA, USA). Polylactic acid (PLA) pellets, grade Ingeo™ 4043D, were provided by NatureWorks LLC (Minnetonka, MN, USA). A Cellic® CTec2 enzymatic cocktail including both cellulolytic and hemicellulolytic activities (specific activity ≥ 1000 U · g^{-1}) was supplied by Novozymes (Bagsvaerd, Denmark) and prepared at 15 FPU · g^{-1} of lignocellulosic biomass for the production of hydrolysates rich in monomeric sugars. The immobilized lipases in acrylic resin (Novozym435®) from *Candida antarctica*, expressed in *Aspergillus niger*, with ≥5000 U · g^{-1} (U: amount of enzyme activity that generates 1 µmol of propyl laurate per minute under standard conditions), were supplied by Sigma-Aldrich (Steinheim, Germany).

2.3. Iono-Organosolv Fractionation: The Coffionic Strategy

Six hundred mg of horse manure was added to 15 mL of 1-ethyl-3-methylimidazolium acetate ([C_2mim][OAc]), corresponding to a concentration of 4% *w*/*v*, and incubated at 110 °C under vigorous magnetic stirring for 40 min. Then, 45 mL of 2-methyltetrahydrofuran-3-one (MeTHF-3-one) was introduced to the system to reach an [C_2mim][OAc]/MeTHF-3-one ratio of 1:3 (*v*/*v*), thereby diluting the biomass to a final concentration of 1% (*w*/*v*).

Glutamic acid was subsequently added to a final concentration of 0.25 M in the reaction medium as in the Coffeecat organosolv process [21]. The set-up was then placed under reflux at 140 °C for 6 h. The operating temperatures used in the Coffionic strategy (110 then 140 °C) were selected based on previous studies demonstrating the thermal stability of both 1-ethyl-3-methylimidazolium acetate and MeTHF-3-one under these conditions [20,21].

Upon completion of the treatment, the mixture was then filtered under vacuum. The retained solid fraction, corresponding to the polysaccharide-rich fraction, was washed with 70% (*v*/*v*) ethanol and subsequently washed with ultrapure water until a whitish-colored solid was obtained. The filtrate, consisting of the [C_2mim][OAc]/MeTHF-3-one solvent mixture containing the dissolved lignin, was subjected to a precipitation step. Three volumes of distilled water (180 mL) were added, and the resulting mixture was heated under reflux at 140 °C for 1 h to promote phase separation. The suspension was then centrifuged, and the recovered lignin was washed repeatedly with distilled water until the conductivity of the washings was below 5 $\mu S \cdot cm^{-1}$ to remove residual ionic liquid. The polysaccharide-rich fraction and lignin were subsequently freeze-dried. The liquid fraction, corresponding to the [C_2mim][OAc]/MeTHF-3-one solvent mixture, was concentrated by rotary evaporation (Büchi Rotavapor R-200, Flawil, Switzerland) to remove water under reduced pressure (72 mbar, 40 °C) and then reused for the next fractionation cycle. The lignin extraction yield obtained after the Coffionic strategy was calculated based on the weight and lignin content of the lignin fraction and horse manure, expressed in % using Equation (1):

$$\text{Acid Insoluble Lignin extraction yield } (\%) = \frac{\text{mass of AIL in lignin fraction(g)}}{\text{mass of AIL in horse manure(g)}} \times 100 \quad (1)$$

2.4. Enzymatic Digestibility of Polysaccharide-Rich Fraction and Methanogenic Potential

Reactions were performed in citrate–phosphate buffer (50 mM, pH 5.0) using the commercial hemicellulolytic enzyme cocktail Cellic® CTec2 (Novozymes, Denmark). The solid substrate was loaded at 4% (*w*/*v*), and the enzyme concentration was 15 FPU $\cdot g^{-1}$ of substrate. Hydrolysis experiments were conducted at 50 °C for 168 h under continuous agitation in 50 mL glass tubes placed in a Carousel 12 Plus Reaction Station™ (Radleys, Saffron Walden, Essex, UK). Aliquots were periodically withdrawn during the kinetic study, centrifuged to remove residual solids, and the supernatants were analyzed by high-performance anion-exchange chromatography with pulsed amperometric detection (HPAEC-PAD) to quantify released monosaccharides. Monomeric sugar yields were expressed as percentages of their initial content in the solid substrate, as defined in Equation (2).

$$\text{Sugar yield } (\%) = \frac{\text{D-Glu or D-Xyl released in hydrolysate(g)}}{\text{D-Glu or D-Xyl content in initial solid(g)}} \times 100 \quad (2)$$

The biochemical methane potential (BMP) of the polysaccharide-rich fraction was determined by Eurofins Ecotoxicologie France SAS (Maxéville, France), following the same experimental protocol as previously applied to raw horse manure in our earlier study [19].

2.5. Enzymatic Transesterification of Lignin and PLA–Lignin Film Tailoring

The lignin functionalization route was adapted from our previous strategies, reported in the literature [24]. Transesterification of Coffionic lignin (1% *w*/*v*, 100 mg) was carried out with ethyl oleate (0.24 M) as acyl donor in MeTHF-3-one (10 mL) and catalyzed by immobilized lipase Novozym435® (10 $g \cdot L^{-1}$). Prior to reaction, substrates, enzyme and solvent were equilibrated under vacuum in a desiccator containing saturated $MgCl_2$ solution for at least 24 h to control water activity (a_w~0.30). Reactions were conducted

in 50 mL glass tubes placed in a Carousel 12 Plus Reaction Station™ (Radleys, Essex, UK) at 75 °C for 48 h under continuous moderate magnetic stirring. At the end of the reaction, the immobilized enzyme was removed by filtration, and the liquid phase was subsequently evaporated under reduced pressure (15 mbar, 60 °C) using a rotary evaporator (Büchi Rotavapor R-200, Flawil, Switzerland). The resulting residue, corresponding to enzymatically modified lignin, was successively washed with hexane and water to remove unreacted ethyl oleate and residual MeTHF-3-one, respectively. The purified product was recovered as a powder after freeze-drying. Control experiments were performed under identical conditions, either in the absence of ethyl oleate or without immobilized lipase. No product was detected in either case.

Extracted lignin and enzymatically modified lignin were subsequently used for the preparation of PLA–lignin films adapted from a previous study [12]. Polylactic acid (PLA, 100 g · L^{-1}) was first dissolved in dichloromethane (DCM) in 50 mL glass tubes placed in a Carousel 12 Plus Reaction Station™ (Radleys, Essex, UK) at 25 °C under vigorous stirring. Separately, lignin or esterified lignin was dissolved in tetrahydrofuran (THF) and then added dropwise to the PLA solution under continuous stirring. The resulting mixture was adjusted to obtain a final PLA/lignin weight ratio of 70/30 *w*/*w*. The resulting mixture was cast into a circular mold and left at room temperature to allow for the complete evaporation of DCM and THF, yielding solid PLA–lignin films.

2.6. Analytical Procedures

The quantification of structural carbohydrates from solid fractions and total sugars from enzymatic hydrolysis supernatants was performed using High-Performance Anion Exchange Chromatography equipped with pulsed amperometric detection (HPAEC-PAD) (Dionex ICS 5000^+ DC, Thermo Fisher Scientific, Waltham, MA, USA) and a CarboPac PA-20 analytical column (3 mm × 150 mm) equipped with a pre-column (3 mm × 30 mm). Elution was performed at 25 °C using a flow rate of 0.5 mL · min^{-1} and a gradient method using Phase A (200 mM NaOH), Phase B (10 mM NaOH) and Phase D (ultra-pure water) [20].

The solid fractions were characterized by infrared spectroscopy using a Shimadzu FTIR 8400 S spectrometer (Shimadzu, Strasbourg, France) in Attenuated Total Reflectance (ATR) analysis mode [20].

The Coffionic lignin was solubilized in DMSO-d_6 (10% *w*/*v*) for 2D NMR studies. The spectra were recorded at 298K on a spectrometer (Bruker Avance III 500, Bruker Corporation, Billerica, MA, USA) equipped with a 5 mm BBI probe operating at 125.7452 MHz (^{13}C channel) and 500.0800 MHz (^{1}H channel). The HSQC cross-signals were assigned, and a semiquantitative analysis of the aromatic region (δ_C/δ_H 100–150 ppm/5.0–9.0 ppm) intensities was performed following the previously reported procedure [25]. The quantification of hydroxyl groups was performed using ^{31}P NMR on the same spectrometer operating at 202.4360 MHz. In total, 60 mg of the sample was solubilized in 350 µL of a pyridine:deuterated chloroform mixture (1.6:1 *v*-*v*), followed by the addition of 100 µL of TMDP and 200 µL of a solution containing 55 mM of N-hydroxyphtalimide (internal standard) and 7.15 mM of chromium acetylacetonate (in pyridine:deuterated chloroform mixture (1.6:1 *v*/*v*)). Samples were centrifuged, and the supernatant was transferred immediately to NMR tubes. The assignment was carried out according to the data in the literature, and the functional OH group was estimated in relative amounts [19,20,26].

The polysaccharide-rich fraction was analyzed by solid-state ^{13}C NMR Cross-Polarization Magic Angle Spinning (CP-MAS), as previously described for cellulose or lignocellulosic biomass [27], using a Bruker Avance III HD 500 spectrometer (Bruker Corporation, Billerica, MA, USA) equipped with a 4 mm CP-MAS probe, operating at 125.7452 MHz (^{13}C) and 500.0800 MHz (^{1}H). Samples were spun at 5 kHz under MAS

conditions at 25 °C. Proton-decoupled ^{13}C NMR spectra were acquired using the Two-Pulse Phase Modulation (TPPM 15) sequence. A total of 10,240 scans were collected with an acquisition time of 27 ms, a contact time of 1 ms, a relaxation delay of 5 s, and a spectral width of 0–298.9366 ppm (37,593.984 Hz) at 25 °C. A line-broadening ("lb") factor of 5 Hz was applied during data processing.

The morphology of the solid fractions and PLA(-lignin) films was characterized using a Quanta 200 FEG Environmental Scanning Electron Microscope (ESEM, Thermo Fisher Scientific, Waltham, MA, USA) according to the analysis conditions described in previous studies [20].

The wettability and surface energy of the PLA films (neat PLA, Coffionic lignin–PLA, esterified lignin–PLA) were analyzed using a Drop Shape Analyzer 25 (Krüss Scientific, Hamburg, Germany). Dynamic contact angles were measured by depositing 20 µL of ultrapure water or diiodomethane via a 0.512 mm stainless steel needle. To eliminate artifacts from local energy minima (static pinning), a tilting-base method was employed [28]. The equilibrium contact angle and the total surface free energy (dispersive and polar components) were calculated using the Owens–Wendt–Rabel–Kaelble (OWRK) method.

Unless otherwise stated, all experiments were performed with at least three independent replicates ($n \geq 3$), and the results are expressed as mean ± standard deviation.

3. Results

3.1. Extraction and Recyclability

Horse manure was processed using the Coffionic strategy, combining treatment with [C_2mim][OAc] and MeTHF-3-one. It was first pretreated with [C_2mim][OAc] before incubation with MeTHF-3-one. The process efficiently separated the biomass into a polysaccharide-rich fraction and a lignin-rich liquid fraction, which was subsequently precipitated, washed, and freeze-dried. This latter fraction was referred to as Coffionic lignin and was recovered with a yield of 30.20 ± 1.10 g per 100 g of initial biomass, while the polysaccharide-rich fraction accounted for 59.30 ± 2.90 g per 100 g (Figure 1).

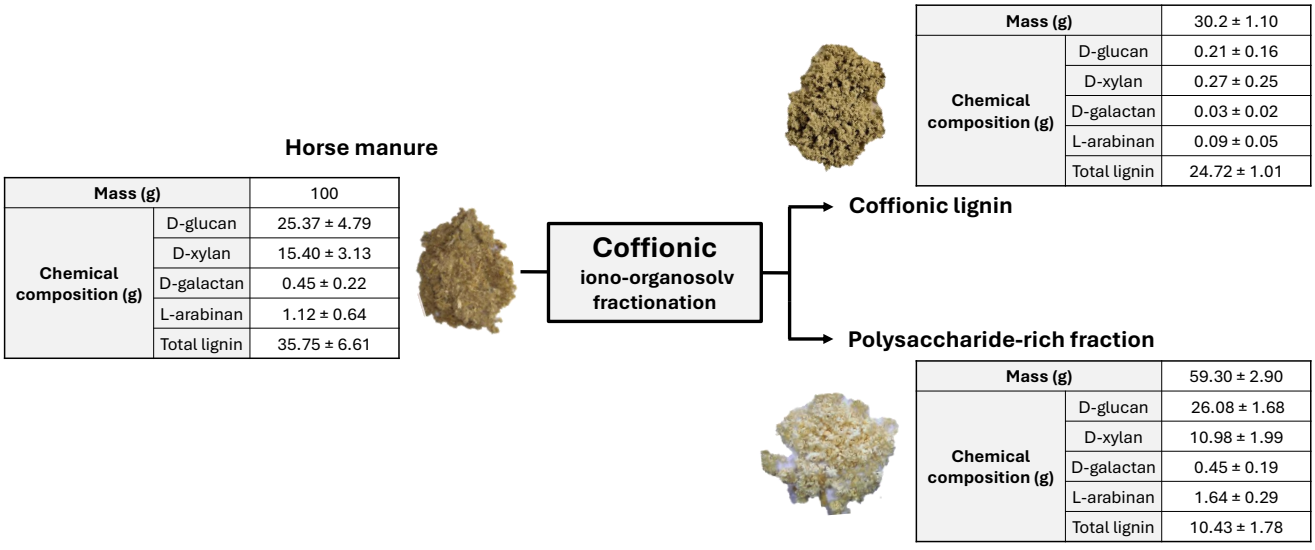

Figure 1. Global mass balance of carbohydrates and total lignin (acid-insoluble plus acid-soluble lignins) after Coffionic strategy applied to horse manure.

The global mass balance showed a loss of 11.5 ± 3.0% *w*/*w*, which was acceptable at the laboratory scale. The global mass balance indicated that almost all the D-glucose and 70% of D-xylan were recovered in the polysaccharide-rich fraction. The remaining D-xylan

was suggested to be solubilized in the [C_2mim][OAc]/MeTHF-3-one mixture, indicating limited depolymerization of hemicelluloses during fractionation. For both, only a residual presence was observed in the Coffionic lignin. Thus, the Coffionic strategy led to a selective extraction of 70% of the total lignin, nearly devoid of sugar.

Notably, the recovery yields remained in the same order of magnitude throughout the four reuses of the [C_2mim][OAc]/MeTHF-3-one mixture in the Coffionic strategy. Table 1 shows the chemical composition of the two fractions following the reuse cycles. The chemical composition of the polysaccharide-rich fraction revealed an efficient delignification even after four cycles, as evidenced by an acid-insoluble lignin content consistently below 15% w/w and a combined D-glucan and D-xylan content superior to 60% w/w. The acid-insoluble lignin content in the Coffionic lignin showed no significant variation over four cycles, remaining stable at an average of 64.3 ± 4.3% w/w. In parallel, the acid-soluble lignin content averaged 13.9 ± 1.6% w/w, while the residual total monosaccharide content remained consistently below 3% w/w.

Table 1. Effect of solvent reuse on the chemical composition (% w/w) of the fractions obtained from Coffionic strategy of horse manure (cycle 1: first use).

Figure	Number of Cycle	Chemical Composition (% *w*/*w*)				
		D-Glucan	D-Xylan	D-Galactan	D-Arabinan	Acid-Insoluble Lignin
Polysaccharide-rich fraction	1	43.98 ± 2.86	18.51 ± 3.37	0.76 ± 0.32	2.77 ± 0.50	10.50 ± 1.01
	4	45.78 ± 0.99	22.15 ± 0.07	0.92 ± 0.09	3.39 ± 0.01	14.87 ± 1.43
Coffionic lignin	1	<3				69.13 ± 1.23
	4	<3				61.14 ± 1.43

3.2. Polysaccharide-Rich Fraction: Characterization and Bioconversion Potential

Figure 2 illustrates the microscopic morphologies of polysaccharide-rich fraction compared to raw horse manure.

The SEM image of raw horse manure (Figure 2A) revealed a compact and granular structure composed of irregular aggregates with minimal fibrillation. Higher magnification (Figure 2B) showed fragmented lamellar elements still embedded within the lignocellulosic matrix. The Coffionic strategy generated a highly fibrillated fraction (Figure 2C,D), with long, thin, and extensively entangled microfibrils.

The solid-state ^{13}C CP-MAS NMR spectrum of the polysaccharide-rich material (Figure 3) exhibited a signal at 105.1 ppm, corresponding to anomeric C1 carbons of glucose, while the intense resonance at 75.2 ppm corresponded to C2, C3 and C5 carbons. The C4 region showed contributions from amorphous cellulose (83.3 ppm) and the crystalline region (89.0 ppm), supporting the presence of a mainly amorphous polysaccharidic framework in this fraction. The C6 signal appeared at 63.7 ppm. Altogether, this spectrum corresponds to cellulose polymer. The contribution of residual lignin in this fraction could not be detected. Likewise, FTIR spectra confirmed substantial delignification, which remained consistent over successive reuse cycles (Figures S1 and S2A).

Based on these structural features, the bioconversion potential of the polysaccharide-rich fraction was subsequently evaluated. The first step was to assess the enzymatic digestibility prior to biochemical methane potential (BMP) determination. Figure 4 presents the kinetics of monosaccharide production over 7 days of hydrolysis, catalyzed by the enzymatic cocktail Cellic® CTec2. The enzymatic hydrolysis of the polysaccharide-rich fraction exhibited rapid sugar release within the first 48 h, reaching a glucose production yield of 75.8 ± 3.3% after 48 h and a total conversion after 7 days (>99%). Xylose was released more gradually and a final yield of 71.7 ± 3.5% as early as 48 h was reached. All

these observations are good indicators of a high enzymatic digestibility of constitutive cellulose and hemicellulose from the polysaccharide-rich fraction.

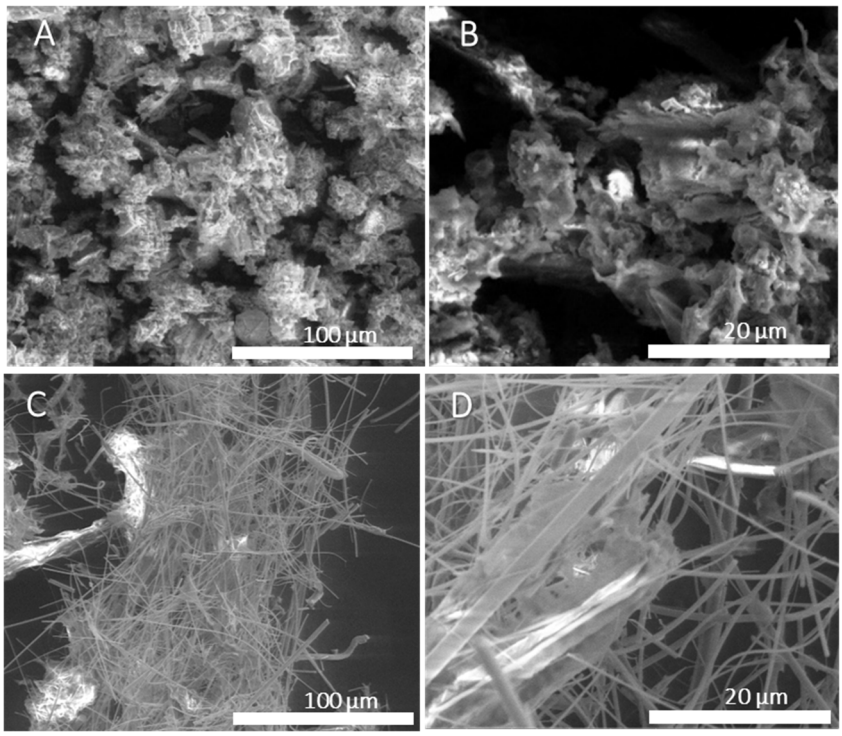

Figure 2. SEM images of raw horse manure (**A**,**B**) and the polysaccharide-rich fraction obtained by Coffionic strategy (**C**,**D**).

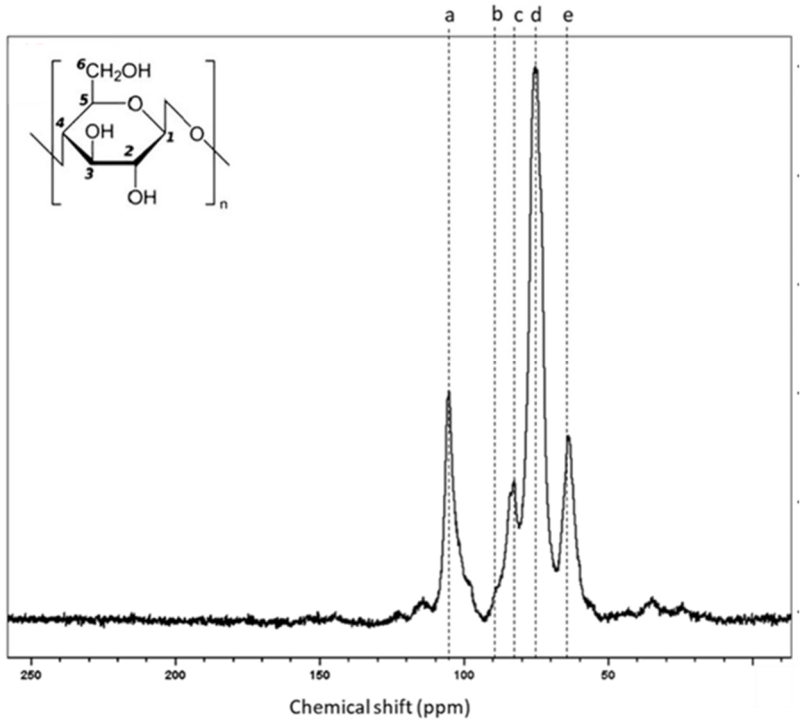

Figure 3. Solid-state CP MAS ^{13}C NMR spectrum of the polysaccharide-rich fraction generated by the Coffionic strategy (a: 105.1 ppm, b: 89.0 ppm, c: 83.3 ppm, d: 75.2 ppm, e: 63.7 ppm).

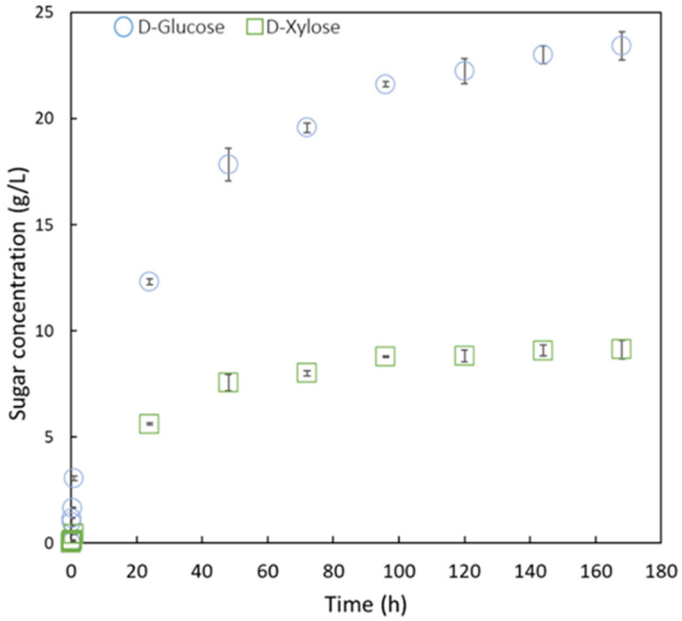

Figure 4. Kinetics of D-glucose and D-xylose release during enzymatic hydrolysis of polysaccharide-rich fraction.

The BMP of the polysaccharide-rich fraction was determined. The produced biogas consisted mainly of methane and carbon dioxide, accounting for 55% v/v and 35% v/v, respectively. The BMP reached 308.77 $\pm$ 5.69 m^3 $CH_4 \cdot t^{-1}$ OM.

3.3. Characterization of the Coffionic Lignin

The properties of the extracted lignin fraction were investigated to assess its suitability for further valorization.

SEM images of the Coffionic lignin (Figure 5) highlight large agglomerates on the order of several micrometers, with some small spherical lignin nanoparticles clustered on the surfaces. The surface morphologies remained largely similar across reuse cycles (Figure S3), indicating that solvent recycling does not significantly affect the morphology of the extracted lignin. The FTIR spectra further showed that, despite a few minor spectral differences, the overall lignin fingerprint was preserved throughout the reuse cycles (Figure S2B).

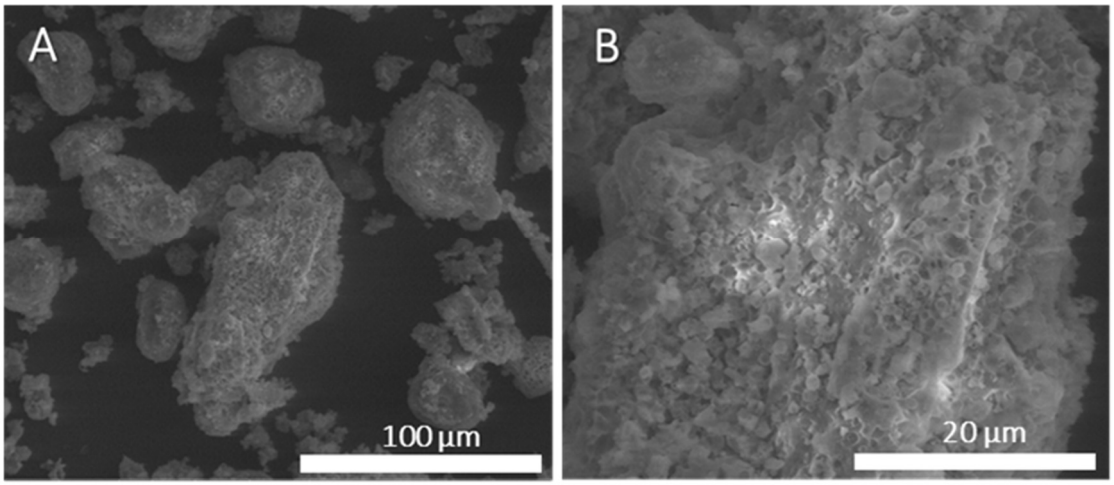

Figure 5. SEM images of Coffionic lignin (**A**,**B**).

The 2D NMR HSQC spectrum of Coffionic lignin revealed distinctive features in both the aromatic (δC/δH 98–132/6.4–8.0 ppm) and side-chain (δC/δH 48–90/2.8–5.2 ppm) regions (Figure 6). In the aromatic region, cross-peaks corresponding to *p*-hydroxyphenyl (H), guaiacyl (G), and syringyl (S) units were observed, with an H/G/S ratio of 2/35/63, indicating a strong dominance of syringyl units.

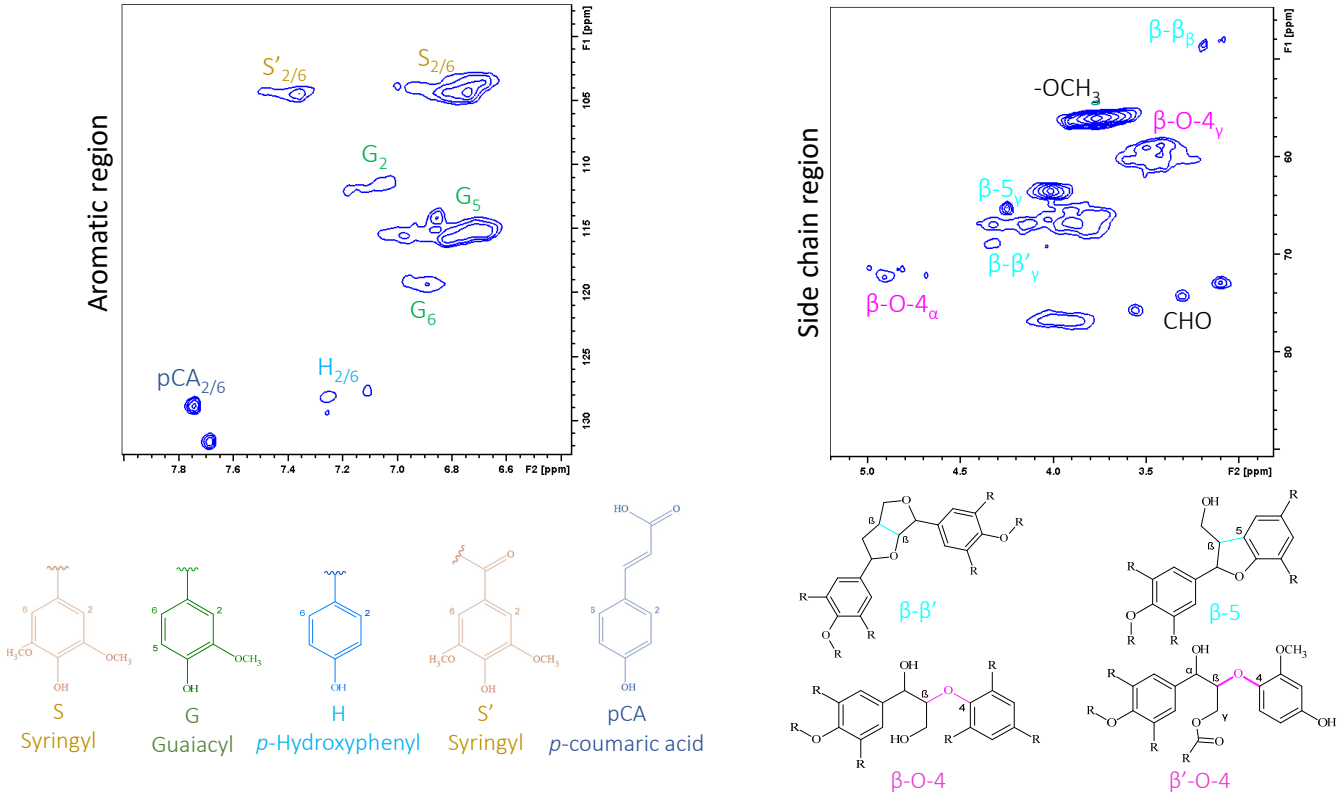

Figure 6. 2D HSQC NMR spectra (aromatic and side-chain regions) of Coffionic lignin. Main interunit linkages, units, and substructures identified from the lignin polymer.

In the side-chain region, methoxy (-OCH_3) substituents were detected, though less pronounced than in other horse manure lignins [19], consistent with very low residual polysaccharide content. The proportion of β-aryl-ether (β-O-4) interunit linkages was estimated at 47%, suggesting a promising preservation of native interunit linkages.

3.4. Enzymatic Esterification of Lignin

We present here, for the first time, an enzymatic strategy in a non-conventional medium for Coffionic lignin esterification in order to modify physicochemical properties (Figure 7).

To ensure adequate substrate availability, lignin was introduced at a concentration of 1% (*w*/*v*), well below its solubility limit in MeTHF-3-one (9.95 ± 0.25 g · L^{-1}) at 75 °C. Figure 8 presents the FTIR spectra of the enzymatically modified lignin and control lignin isolated after 72 h of incubation in the reaction medium without the enzyme. The characteristic bands of the control lignin spectrum were less well resolved but remained consistent with those of the Coffionic lignin (Figure S2).

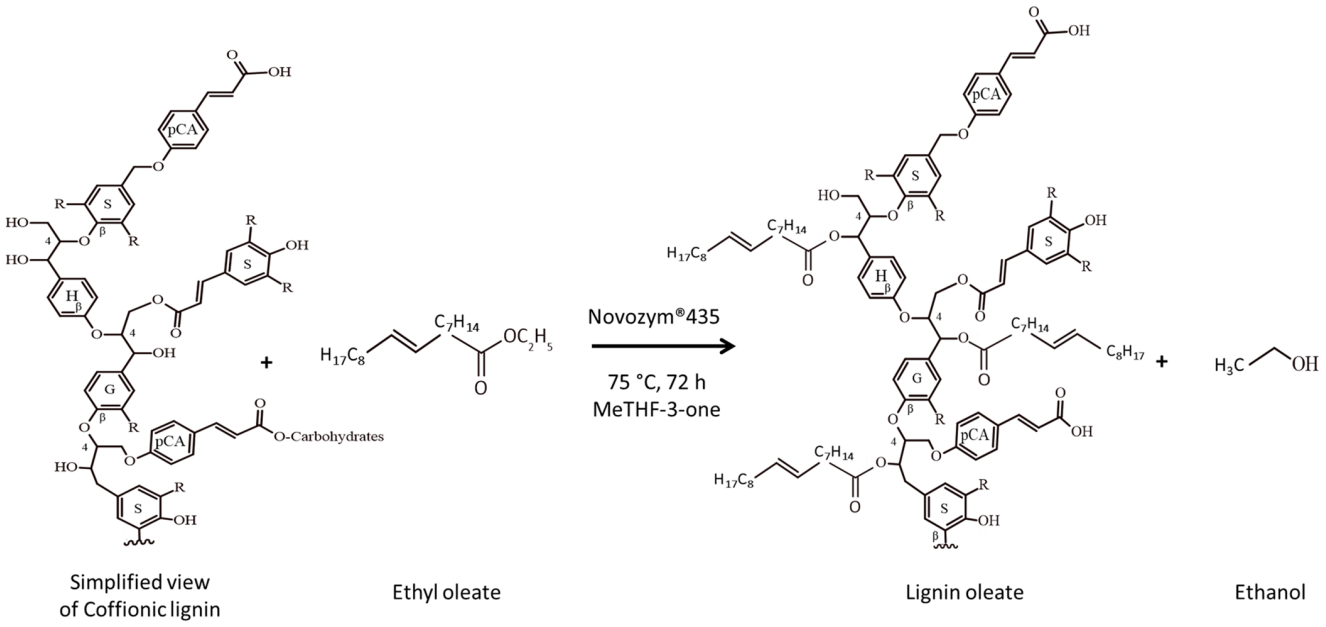

Figure 7. Reaction scheme of Novozym435®-catalyzed transesterification of Coffionic lignin with ethyl oleate as the acyl donor in 2-methyltetrahydrofuran-3-one (MeTHF-3-one). Coffionic lignin was represented in a simplified form based on the calculated H/G/S ratio of 2/35/63.

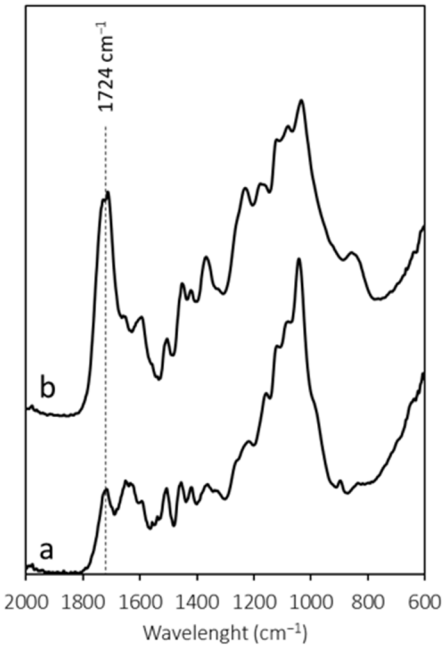

Figure 8. FTIR spectra in the range of 2000 to 600 cm^{-1} of control lignin isolated by evaporation from the reaction medium without enzyme (**a**) and modified lignin isolated by evaporation from the reaction medium after transesterification catalyzed by Novozym435® (**b**).

This indicated that incubation in the absence of enzyme induced only minor structural changes. A similar weak band at 1724 cm^{-1}, assigned to the ester C=O stretching vibration [29], is observed in both the control (Figure 8) and Coffionic lignin (Figure S2) spectra. This confirmed the efficiency of the washing steps and rules out ethyl oleate adsorption effects. By contrast, the lignin modified after 72 h of reaction exhibited a pronounced band at 1724 cm^{-1} in favor of the formation of ester linkages through enzymatic catalysis [30]. To confirm the success of the transesterification and elucidate the regioselectivity of the reaction, ^{31}P NMR analysis was performed on the Coffionic lignin before and

after enzymatic transesterification (Figure S3). The quantitative analysis of the hydroxyls of both Coffionic and modified lignins was summarized in Table 2.

Table 2. Quantification by ^{31}P NMR of hydroxyl groups of Coffionic lignin before and after enzymatic transesterification.

Chemical Shift (ppm).	Assignment	Content (mmol · g^{-1})	
		Coffionic Lignin	Esterified Lignin
146.0–149.2	Aliphatic -OH	1.90 ± 0.45	1.29 ± 0.10
137.7–144.0	Phenolic -OH	0.49 ± 0.10	0.51 ± 0.05
Total -OH		2.39 ± 0.16	1.80 ± 0.06
133.6–136.0	Carboxylic -OH	0.29 ± 0.09	1.13 ± 0.03

Coffionic lignin prior to transesterification displayed a marked predominance of aliphatic hydroxyl groups (1.90 ± 0.45 mmol · g^{-1}) relative to phenolic hydroxyls (0.49 ± 0.10 mmol · g^{-1}), which is consistent with a high degree of preservation of aryl ether linkages within the polymer backbone [31]. Upon enzymatic transesterification, the aliphatic hydroxyl content decreases to 1.29 ± 0.10 mmol · g^{-1}, whereas the phenolic hydroxyl content remains essentially unchanged (0.51 ± 0.05 mmol · g^{-1}). This result clearly demonstrates the strong regioselectivity of the Novozym435®-catalyzed reaction toward aliphatic hydroxyl groups, corresponding to an overall conversion yield of 32%. The increase in carboxylic hydroxyl groups after functionalization may arise either from residual oleic acid produced by undesirable partial ethyl oleate hydrolysis (Hulin et al., 2015) or from lipase-mediated hydrolysis of ester linkages in residual lignin–polysaccharide complexes, given the substrate versatility of this enzyme [32].

3.5. Wettability and Surface Energy of PLA–Lignin Films

The impact of this selective modification on lignin–PLA interactions in tailored films was then evaluated. PLA films with and without lignin were prepared by solvent casting. Neat PLA (Figure 9a) films are transparent and colorless, exhibiting a smooth and homogeneous appearance. Figure 9b shows that the incorporation of Coffionic lignin imparted a characteristic brown coloration to the films, with the PLA–lignin sample appearing darker and less transparent [33,34]. Films containing esterified lignin displayed a more uniform and glossier surface, with a lighter brown tone and a clearly flexible appearance (Figure 9c). Dynamic contact angle measurements using water and diiodomethane were used to evaluate the impact of Coffionic lignin or esterified lignin incorporation on the apolarity properties of PLA-based films (Table 3). Neat PLA exhibits moderate wettability, with an equilibrium water contact angle of 55.7° and a diiodomethane contact angle of 38.6°, corresponding to a total surface energy of 52.7 mN · m^{-1} dominated by dispersive interactions [33,34]. This behavior is consistent with the smooth and homogeneous surface observed by SEM (Figure 9A,D).

The incorporation of Coffionic lignin induced heterogeneous and porous morphology (Figure 9B,E), suggesting phase separation and lignin aggregation at the film surface. This behavior can be attributed to the high accessibility of aliphatic and phenolic hydroxyl groups preserved during the Coffionic strategy as evidenced by ^{31}P NMR analyses. However, it also highlights the intrinsic polarity of Coffionic lignin, which limits its compatibility with PLA. Moreover, the increase in water contact angle to 58.7° and the diiodomethane contact angle to 56.7° indicated reduced dispersive interactions and weaker interfacial affinity.

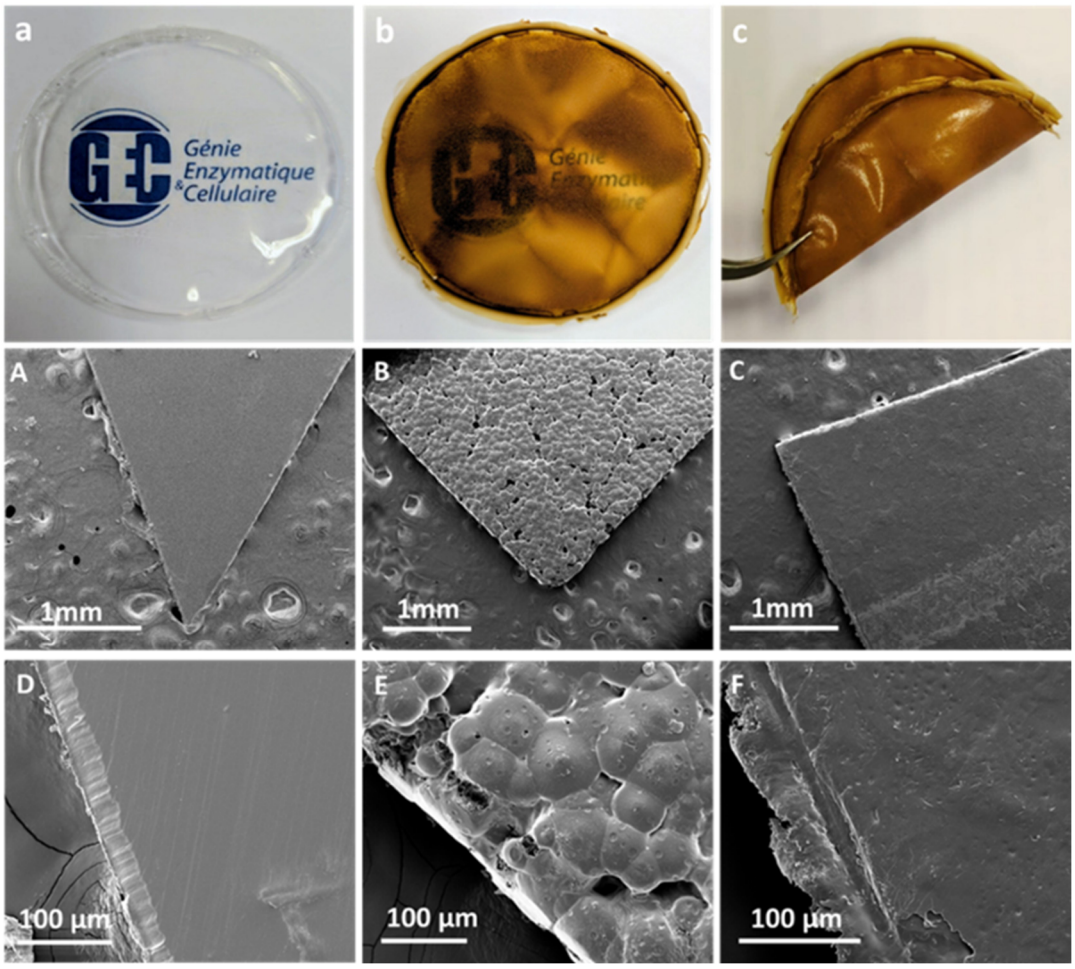

Figure 9. Visual comparison/SEM images of neat PLA (**a**,**A**,**D**) and PLA films containing unmodified (**b**,**B**,**E**) and esterified lignin (**c**,**C**,**F**) at 30% *w*/*w*.

Table 3. Water and diiodomethane contact angles and corresponding polar and dispersive surface energies of neat PLA, PLA–lignin, and PLA–esterified lignin films.

Tailored PLA–Based Films	PLA (100% *w*/*w*)	PLA–Coffionic Lignin (70/30% *w*/*w*)	PLA–Esterified Lignin (70/30% *w*/*w*)
Water contact angle (°)	55.68 ± 0.25	58.7 ± 0.25	82.34 ± 0.41
Diiodomethane contact angle (°)	38.61 ± 1.18	56.69 ± 2.68	30.76 ± 2.11
Polar surface energy (mN · m^{-1})	12.44 ± 0.41	15.42 ± 0.73	24.06 ± 1.66
Dispersive surface energy (mN · m^{-1})	40.30 ± 1.33	30.48 ± 1.45	43.90 ± 3.03
Total surface energy (mN · m^{-1})	52.74 ± 0.87	45.90 ± 1.09	67.97 ± 2.34

In contrast, PLA films containing enzymatically esterified lignin exhibit a pronounced increase in apolarity, with an equilibrium water contact angle of 82.4°, together with a strong decrease in the diiodomethane contact angle to 30.8°. This shift reflects enhanced dispersive interactions, as confirmed by the increase in dispersive surface energy to 43.9 mN · m^{-1} and a total surface energy of 68.0 mN · m^{-1}. SEM observations (Figure 9C,F) revealed a compact and homogeneous surface morphology, closely resembling that of neat PLA, indicating improved lignin dispersion and interfacial adhesion.

4. Discussion

According to the chemical composition results, horse manure is a suitable feedstock for the integrated valorization of polysaccharides and lignin, regardless of storage conditions, contamination, or sample variability [3,7,19]. The aim of our study was to preserve or improve the bioconversion potential of the polysaccharide fraction while isolating a valuable lignin fraction free of sugar. To this end, an iono-organosolv strategy was undertaken to combine the ability of ionic liquid to generate a highly digestible polysaccharide fraction and the ability of the organosolv strategy to isolate a lignin fraction with retained aryl-ether interunit linkages [16,20,35]. The global mass balance provides valuable data on the validity of this fractionation and highlights the achievement of lignin extraction performance that is particularly competitive and selective compared with other approaches reported in the literature [36–38]. The polysaccharide-rich fraction obtained with the Coffionic strategy exhibited greater glucan and xylan enrichment than those obtained with single IL or organosolv pretreatments [20,21]. Although the choices of solvents are also based on sustainability considerations, their respective cost could hinder development if not recycled. However, reusing solvents in organosolv or ionosolv fractionation often leads to reduced delignification due to the accumulation of biomass-derived impurities such as hemicellulose sugars, low-molecular-weight lignin fragments and phenolics [20,39,40]. This is the reason why their reuse was investigated. In this study, the results confirm the satisfactory selective extraction of lignin from horse manure, yielding a maintained purity of 78.1% w/w after four solvent reuse cycles. The stable performance observed over four reuse cycles supports the feasibility of solvent recycling. Future work will complement these performance indicators by more finely monitoring the composition and structural integrity of the recycled solvent system to better define solvent lifetimes under scale-up conditions. As this work represents a first feasibility study, further investigations will also address the versatility of the strategy using horse manure from different origins, as well as solvent recovery, energy demand and solvent cost under pilot-scale conditions.

The morphological SEM analyses of the polysaccharide-rich fraction reflect efficient delignification, consistent with chemical composition data and the absence of severe fiber disruption and surface erosion commonly reported after single organosolv or IL pretreatments [19,41]. The structural analysis using solid-state NMR and FTIR (Figure S1) clearly evidences the characteristic of mainly amorphous cellulose and hemicellulose [27], constituting a relevant indicator for further enzymatic depolymerization, which constitutes one of the main bottlenecks in the anaerobic digestion of horse manure into methane [42]. The enzymatic hydrolysis of this fraction led to highly effective carbohydrate hydrolysis, markedly superior to that of untreated (< 10%), ionic liquid-pretreated (56.4 $\pm$ 0.7%) or organosolv-pretreated horse manures at the same time point [19]. Overall, these results make downstream anaerobic digestion a viable option. The obtained polysaccharide-rich fraction led to a BMP improvement of approximately 17% compared to untreated horse manure. This BMP is similar to the one obtained after single ionic liquid pretreatment and higher than after the organosolv process or ball milling [7,19,43].

In SEM images, Coffionic lignin typically appears as micrometer-scale particles, an effect commonly linked to its strong tendency to self-associate during the precipitation or drying steps [31]. This morphology, together with a largely unchanged FTIR spectral fingerprint over successive reuse cycles (Figures S2B and S3), suggests that the structural characteristics of the Coffionic lignin and the fractionation performance can be maintained throughout solvent mixture reuse. The 2D NMR HSQC spectrum reveals a high proportion of β-aryl-ether (β -O-4) linkages (~47%), which ranges intermediately between milled wood lignin (~75%) and soda lignin from wheat straw (~30%) [44,45]. Interestingly, the Coffionic strategy can reach higher β-aryl-ether linkage content than single ionic liquid or organosolv

pretreatments at around 35–37% [19]. This result would imply persistent aliphatic hydroxyl group content in the polymer available for further enzymatic esterification.

Thus, the reaction was catalyzed by Novozym435®, an immobilized enzyme of industrial interest, and carried out in MeTHF-3-one, a food-grade and biodegradable solvent previously used for lignin extraction, enhancing the circularity of our integrated approach. Ethyl oleate was selected as the natural acyl donor, chosen for its ability to increase the apolarity of biomolecules and biopolymers [24]. The regioselectivity of the enzymatic esterification is exclusively directed toward aliphatic hydroxyl groups of lignin, leaving free phenolic hydroxyl groups preserving intrinsic physicochemical and biological properties for lignin-based material tailoring (such as anti-UV or antimicrobial activities) [46]. Previous studies have reported that esterification can improve lignin's compatibility with PLA, leading to better dispersion and improved composite properties [47,48]. Therefore, the impact of oleyl chain grafting to aliphatic hydroxyl groups was then assessed in terms of compatibility in the PLA matrix. The results suggest that enzymatic transesterification efficiently masks the polar hydroxyl groups of the lignin polymer, thereby improving its interfacial compatibility with the PLA matrix. Overall, the correlation between surface energetics and morphology suggests that this selective and green enzymatic route improves PLA–lignin interfacial interactions. Such control over surface homogeneity and dispersive interactions is particularly advantageous for fused filament fabrication, where stable extrusion, interlayer adhesion and print quality are governed by both surface energy and microstructural continuity [12].

5. Conclusions

This work demonstrates that the Coffionic iono-organosolv strategy is an effective approach to the fractionation of horse manure, enabling both improved methane production and the recovery of a lignin fraction suitable for further valorization. Compared with the single ionosolv or organosolv pretreatments reported in the literature, this strategy offers a balanced compromise between lignin extraction yield, low residual sugar content and preservation of polymeric features while maintaining performance upon solvent reuse. The enhanced enzymatic digestibility of the polysaccharide-rich fraction results in a higher biochemical methane potential than most previously reported pretreatments for horse manure. In parallel, the extracted lignin can be selectively modified by enzymatic transesterification in a food-grade solvent and successfully incorporated into PLA to form flexible, homogeneous and more hydrophobic films. Importantly, efficient solvent recovery and reuse further support the environmental sustainability of the Coffionic strategy. Overall, this fractionation strategy, associated with biocatalysis in non-conventional media, provides an integrated and sustainable option for improving the valorization of livestock waste within emerging manure biorefinery concepts.

Supplementary Materials: The following supporting information can be downloaded at https://www.mdpi.com/article/10.3390/bioresourbioprod2030016/s1: Figure S1: Full-range (A) and zoom (B) FTIR spectra of raw horse manure (1) compared to those of polysaccharide-rich fraction (2) and Coffionic lignin (3). Band assignments are based on literature data [20–22]. Figure S2: Effect of solvent reuse cycle on FTIR spectral fingerprints of polysaccharide-rich fraction (A) and Coffionic lignin (B) obtained via the Coffionic strategy: (a) cycle 1, (b) cycle 2, (c) cycle 4. Figure S3: Effect of solvent reuse cycle on morphological properties of lignin fraction extracted by the Coffionic strategy. (A,B) Cycle 1, (C,D) cycle 2, (E,F) cycle 4. Figure S4: ^{31}P NMR spectra of Coffionic lignin before and after enzymatic transesterification, following derivatization with 2-chloro-4,4,5,5-tetramethyl-1,3,2-dioxaphospholane (TMDP).

Author Contributions: L.D.P., A.C., F.T.R., A.B. and S.E.M.E.A.: formal analysis, investigation, methodology. A.J., D.M. and L.D.: methodology, formal analysis. C.S.: data curation, formal analysis, writing—review and editing, conceptualization, funding acquisition, supervision. C.H.: formal analysis, investigation, methodology, conceptualization, writing—review and editing. E.H.: conceptualization, resources, supervision, data curation, validation, formal analysis, writing—original draft, writing—review and editing, funding acquisition. All authors have read and agreed to the published version of the manuscript.

Funding: The authors are grateful for the financial support from Hauts-de-France regional council in developing the STimule program—MoLiMat3D project (2024–2027). Lindsay Dorschner Pelcoq, PhD, was funded by the Hauts-de-France regional council, the Université de Picardie Jules Verne, and SAS Equi-énergies. Asmina Chanfiou (PhD student) was funded by the Hauts-de-France regional council and the Université de Picardie Jules Verne. Fenosoa Tatiana Randremahitsimanana (PhD student) was funded by the France Excellence Eiffel program.

Institutional Review Board Statement: Not applicable.

Informed Consent Statement: Not applicable.

Data Availability Statement: The data supporting this article are included within the article and its Supplementary Information. Additional raw data are available from the corresponding author upon reasonable request.

Acknowledgments: The authors thank SAS Equi-énergies (Coye-la-Forêt, France), a company represented by Bruno Battistini, which specializes in the treatment and recovery of non-hazardous waste, such as the methanization of horse manure. That company was responsible for collecting and making the raw horse manure available. Generative AI was used to design the graphical abstract; the authors take full responsibility for its content.

Conflicts of Interest: The authors declare no conflicts of interest.

References

1. He, X.; Wang, Y.; Zhang, Y.; Wang, C.; Yu, J.; Ohtake, H.; Zhang, T. The potential for livestock manure valorization and phosphorus recovery by hydrothermal technology—A critical review. *Mater. Sci. Energy Technol.* **2023**, *6*, 94–104. [CrossRef]
2. Yildirim, F.; Açar, Y. Value of horse manure for renewable energy production: Anaerobic digestion, biogas generation, and contributions to sustainable development. *Online J. Anim. Feed Res.* **2024**, *14*, 358–366. [CrossRef]
3. Caro, S.; Dahl, O. Thermochemical valorisation of waste: Pyrolytic conversion of horse manure. *Clean. Eng. Technol.* **2021**, *4*, 100181. [CrossRef]
4. Havukainen, J.; Väisänen, S.; Rantala, T.; Saunila, M.; Ukko, J. Environmental impacts of manure management based on life cycle assessment approach. *J. Clean. Prod.* **2020**, *264*, 121576. [CrossRef]
5. Weiland, K.; Alge, K.; Mautner, A.; Bauer, A.; Bismarck, A. Horse manure as resource for biogas and nanolignocellulosic fibres. *Bioresour. Technol.* **2023**, *372*, 128688. [CrossRef] [PubMed]
6. Chong, C.T.; Mong, G.R.; Ng, J.-H.; Chong, W.W.F.; Ani, F.N.; Lam, S.S.; Ong, H.C. Pyrolysis characteristics and kinetic studies of horse manure using thermogravimetric analysis. *Energy Convers. Manag.* **2019**, *180*, 1260–1267. [CrossRef]
7. Naji, A.; Rechdaoui, S.G.; Jabagi, E.; Lacroix, C.; Azimi, S.; Rocher, V. Horse Manure and Lignocellulosic Biomass Characterization as Methane Production Substrates. *Fermentation* **2023**, *9*, 580. [CrossRef]
8. Martínez-Mendoza, L.J.; Múñoz, R.; García-Depraect, O. Enhanced methane production from food waste: A systematic comparison between conventional single-stage and lactate-based two-stage anaerobic digestion processes. *Biomass Bioenergy* **2024**, *188*, 107312. [CrossRef]
9. Nilza, N.; Salam, M.D. Recent advances in generation of bioproducts from lignin: A comprehensive review. *Discov. Sustain.* **2025**, *6*, 1083. [CrossRef]
10. Schröder, A.; Wu, R.; Eklund, P.; Grénman, H.; Xu, C. Active lignin stabilization in lignocellulosic biomass fractionation: Mechanisms and advancements. *Green Chem.* **2026**, *28*, 6562–6584. [CrossRef]
11. Ye, H.; You, T.; Nawaz, H.; Xu, F. A comprehensive review on polylactic acid/lignin composites—Structure, synthesis, performance, compatibilization, and applications. *Int. J. Biol. Macromol.* **2024**, *280*, 135886. [CrossRef] [PubMed]
12. Mohan, M.K.; Krasnou, I.; Lukk, T.; Karpichev, Y. Novel Softwood Lignin Esters as Advanced Filler to PLA for 3D Printing. *ACS Omega* **2024**, *9*, 44559–44567. [CrossRef] [PubMed]

13. Libretti, C.; Santos Correa, L.; Meier, M.A.R. From waste to resource: Advancements in sustainable lignin modification. *Green Chem.* **2024**, *26*, 4358–4386. [CrossRef]
14. Luo, S.; Cao, J.; McDonald, A.G. Esterification of industrial lignin and its effect on the resulting poly(3-hydroxybutyrate-co-3-hydroxyvalerate) or polypropylene blends. *Ind. Crops Prod.* **2017**, *97*, 281–291. [CrossRef]
15. Weißbach, U.; Dabral, S.; Konnert, L.; Bolm, C.; Hernández, J.G. Selective enzymatic esterification of lignin model compounds in the ball mill. *Beilstein J. Org. Chem.* **2017**, *13*, 1788–1795. [CrossRef] [PubMed]
16. Alam, M.M.; Greco, A.; Rajabimashhadi, Z.; Esposito Corcione, C. Efficient and environmentally friendly techniques for extracting lignin from lignocellulose biomass and subsequent uses: A review. *Clean. Mater.* **2024**, *13*, 100253. [CrossRef]
17. Argyropoulos, D.D.S.; Crestini, C.; Dahlstrand, C.; Furusjö, E.; Gioia, C.; Jedvert, K.; Henriksson, G.; Hulteberg, C.; Lawoko, M.; Pierrou, C.; et al. Kraft Lignin: A Valuable, Sustainable Resource, Opportunities and Challenges. *ChemSusChem* **2023**, *16*, e202300492. [CrossRef] [PubMed]
18. Liu, Y.; Zheng, J.; Xiao, J.; He, X.; Zhang, K.; Yuan, S.; Peng, Z.; Chen, Z.; Lin, X. Enhanced Enzymatic Hydrolysis and Lignin Extraction of Wheat Straw by Triethylbenzyl Ammonium Chloride/Lactic Acid-Based Deep Eutectic Solvent Pretreatment. *ACS Omega* **2019**, *4*, 19829–19839. [CrossRef] [PubMed]
19. Pelcoq, L.D.; Dumont, C.; Richard, T.; Jamali, A.; Sauthier, M.; Sarazin, C.; Husson, E. Ionic liquid and organosolv pretreatments of horse manure: Impact on lignin telomerization by organometallic catalysis and methanization. *Biomass Convers. Biorefinery* **2025**, *15*, 15261–15276. [CrossRef]
20. Quesada-Salas, M.C.; Vuillemin, M.E.; Dillies, J.; Dauwe, R.; Firdaous, L.; Bigan, M.; Lambertyn, V.; Cailleu, D.; Jamali, A.; Froidevaux, R.; et al. 1-ethyl-3-methyl imidazolium acetate, hemicellulolytic enzymes and laccase-mediator system: Toward an integrated co-valorization of polysaccharides and lignin from Miscanthus. *Ind. Crops Prod.* **2023**, *197*, 116627. [CrossRef]
21. Vuillemin, M.E.; Quesada-Salas, M.C.; Hadad, C.; Jasniewski, J.; Husson, E.; Sarazin, C. Revisiting organosolv strategies for sustainable extraction of valuable lignin: The CoffeeCat process. *RSC Sustain.* **2023**, *1*, 853–865. [CrossRef]
22. Grande, P.M.; Viell, J.; Theyssen, N.; Marquardt, W.; Domínguez de María, P.; Leitner, W. Fractionation of lignocellulosic biomass using the OrganoCat process. *Green Chem.* **2015**, *17*, 3533–3539. [CrossRef]
23. Sluiter, A.D.; Hames, B.R.; Ruiz, R.O.; Scarlata, C.J.; Sluiter, J.; Templeton, D.W.; Crocker, D.P. *Determination of Structural Carbohydrates and Lignin in Biomass: Laboratory Analytical Procedure (LAP)*; Technical Report NREL/TP-510-42618; National Renewable Energy Laboratory: Golden, CO, USA, 2012.
24. Vuillemin, M.E.; Husson, E.; Laclef, S.; Jamali, A.; Lambertyn, V.; Pilard, S.; Cailleu, D.; Sarazin, C. Improving the environmental compatibility of enzymatic synthesis of sugar-based surfactants using green reaction media. *Process Biochem.* **2022**, *117*, 30–41. [CrossRef]
25. Zijlstra, D.S.; Lahive, C.W.; Analbers, C.A.; Figueirêdo, M.B.; Wang, Z.; Lancefield, C.S.; Deuss, P.J. Mild Organosolv Lignin Extraction with Alcohols: The Importance of Benzylic Alkoxylation. *ACS Sustain. Chem. Eng.* **2020**, *8*, 5119–5131. [CrossRef]
26. Argyropoulos, D.S.; Pajer, N.; Crestini, C. Quantitative 31P NMR Analysis of Lignins and Tannins. *J. Vis. Exp.* **2021**, *174*, e62696. [CrossRef] [PubMed]
27. Husson, E.; Buchoux, S.; Avondo, C.; Cailleu, D.; Djellab, K.; Gosselin, I.; Wattraint, O.; Sarazin, C. Enzymatic hydrolysis of ionic liquid-pretreated celluloses: Contribution of CP-MAS 13C NMR and SEM. *Bioresour. Technol.* **2011**, *102*, 7335–7342. [CrossRef] [PubMed]
28. Tadmor, R. Line Energy and the Relation between Advancing, Receding, and Young Contact Angles. *Langmuir* **2004**, *20*, 7659–7664. [CrossRef] [PubMed]
29. Thielemans, W.; Wool, R.P. Lignin Esters for Use in Unsaturated Thermosets: Lignin Modification and Solubility Modeling. *Biomacromolecules* **2005**, *6*, 1895–1905. [CrossRef] [PubMed]
30. Martinez-Garcia, M.; Gracia-Vitoria, J.; Vanbroekhoven, K.; Dejonghe, W.; Satyawali, Y. Selective Enzymatic Esterification of Lignin-Derived Phenolics for the Synthesis of Lipophilic Antioxidants. *Antioxidants* **2023**, *12*, 657. [CrossRef] [PubMed]
31. Pylypchuk, I.V.; Karlsson, M.; Lindén, P.A.; Lindström, M.E.; Elder, T.; Sevastyanova, O.; Lawoko, M. Molecular understanding of the morphology and properties of lignin nanoparticles: Unravelling the potential for tailored applications. *Green Chem.* **2023**, *25*, 4415–4428. [CrossRef] [PubMed]
32. Rodrigues, R.C.; Virgen-Ortíz, J.J.; dos Santos, J.C.S.; Berenguer-Murcia, Á.; Alcantara, A.R.; Barbosa, O.; Ortiz, C.; Fernandez-Lafuente, R. Immobilization of lipases on hydrophobic supports: Immobilization mechanism, advantages, problems, and solutions. *Biotechnol. Adv.* **2019**, *37*, 746–770. [CrossRef] [PubMed]
33. Makri, S.P.; Xanthopoulou, E.; Klonos, P.A.; Grigoropoulos, A.; Kyritsis, A.; Tsachouridis, K.; Anastasiou, A.; Deligkiozi, I.; Nikolaidis, N.; Bikiaris, D.N. Effect of Micro- and Nano-Lignin on the Thermal, Mechanical, and Antioxidant Properties of Biobased PLA–Lignin Composite Films. *Polymers* **2022**, *14*, 5274. [CrossRef] [PubMed]
34. Makri, S.P.; Xanthopoulou, E.; Valera, M.A.; Mangas, A.; Marra, G.; Ruiz, V.; Koltsakidis, S.; Tzetzis, D.; Zoikis Karathanasis, A.; Deligkiozi, I.; et al. Poly(Lactic Acid) Composites with Lignin and Nanolignin Synthesized by In Situ Reactive Processing. *Polymers* **2023**, *15*, 2386. [CrossRef] [PubMed]

35. Chen, M.; Malaret, F.; Firth, A.E.J.; Verdía, P.; Abouelela, A.R.; Chen, Y.; Hallett, J.P. Design of a combined ionosolv-organosolv biomass fractionation process for biofuel production and high value-added lignin valorisation. *Green Chem.* **2020**, *22*, 5161–5178. [CrossRef]
36. Tian, D.; Chandra, R.P.; Lee, J.-S.; Lu, C.; Saddler, J.N. A comparison of various lignin-extraction methods to enhance the accessibility and ease of enzymatic hydrolysis of the cellulosic component of steam-pretreated poplar. *Biotechnol. Biofuels* **2017**, *10*, 157. [CrossRef] [PubMed]
37. Melikoglu, M. Organosolv lignin: A comprehensive review of pretreatment advancements and biorefinery integration. *Next Mater.* **2025**, *9*, 101136. [CrossRef]
38. Ovejero-Pérez, A.; Rigual, V.; Domínguez, J.C.; Alonso, M.V.; Oliet, M.; Rodriguez, F. Organosolv and ionosolv processes for autohydrolyzed poplar fractionation: Lignin recovery and characterization. *Int. J. Biol. Macromol.* **2022**, *197*, 131–140. [CrossRef] [PubMed]
39. Rahman, M.M.; Choudhary, H.; Simmons, B.A.; Gladden, J.M.; Rodriguez, A. Advances in ionic liquid recycling for lignocellulosic biomass pretreatment. *Green Chem.* **2025**, *27*, 15338–15373. [CrossRef]
40. Rabelo, S.C.; Nakasu, P.Y.S.; Scopel, E.; Araújo, M.F.; Cardoso, L.H.; Costa, A.C.D. Organosolv pretreatment for biorefineries: Current status, perspectives, and challenges. *Bioresour. Technol.* **2023**, *369*, 128331. [CrossRef] [PubMed]
41. Alves, M.D.S.; Rodrigues, P.D.O.; Baffi, M.A.; Pasquini, D. Organosolv and Hydrothermal Pretreatments of Sugarcane Bagasse and Straw and Enzymatic Hydrolysis of Hemicellulosic Liquor. *Fermentation* **2025**, *11*, 550. [CrossRef]
42. Paudel, S.R.; Banjara, S.P.; Choi, O.K.; Park, K.Y.; Kim, Y.M.; Lee, J.W. Pretreatment of agricultural biomass for anaerobic digestion: Current state and challenges. *Bioresour. Technol.* **2017**, *245*, 1194–1205. [CrossRef] [PubMed]
43. Heller, R.; Roth, P.; Hülsemann, B.; Böttinger, S.; Lemmer, A.; Oechsner, H. Effects of Pretreatment with a Ball Mill on Methane Yield of Horse Manure. *Waste Biomass Valorization* **2023**, *14*, 3723–3737. [CrossRef]
44. del Río, J.C.; Rencoret, J.; Prinsen, P.; Martínez, Á.T.; Ralph, J.; Gutiérrez, A. Structural Characterization of Wheat Straw Lignin as Revealed by Analytical Pyrolysis, 2D-NMR, and Reductive Cleavage Methods. *J. Agric. Food Chem.* **2012**, *60*, 5922–5935. [CrossRef] [PubMed]
45. Yang, H.; Xie, Y.; Zheng, X.; Pu, Y.; Huang, F.; Meng, X.; Wu, W.; Ragauskas, A.; Yao, L. Comparative study of lignin characteristics from wheat straw obtained by soda-AQ and kraft pretreatment and effect on the following enzymatic hydrolysis process. *Bioresour. Technol.* **2016**, *207*, 361–369. [CrossRef] [PubMed]
46. Sadeghifar, H.; Ragauskas, A. Lignin as a bioactive polymer and heavy metal absorber—An overview. *Chemosphere* **2022**, *309*, 136564. [CrossRef] [PubMed]
47. Park, C.-W.; Han, S.-Y.; Bandi, R.; Dadigala, R.; Lee, E.-A.; Kim, J.-K.; Cindradewi, A.W.; Kwon, G.-J.; Lee, S.-H. Esterification of Lignin Isolated by Deep Eutectic Solvent Using Fatty Acid Chloride, and Its Composite Film with Poly(lactic acid). *Polymers* **2021**, *13*, 2149. [CrossRef] [PubMed]
48. Shi, K.; Liu, G.; Sun, H.; Weng, Y. Polylactic Acid/Lignin Composites: A Review. *Polymers* **2023**, *15*, 2807. [CrossRef] [PubMed]